Arylthioindole Inhibitors of Tubulin Polymerization. 3. Biological Evaluation, Structure−Activity Relationships and Molecular Modeling Studies

Giuseppe La Regina,[†,‡] Michael C. Edler,[§] Andrea Brancale,[∥] Sahar Kandil,[∥] Antonio Coluccia,[†] Francesco Piscitelli,[†] Ernest Hamel,[§] Gabriella De Martino,[†] Ruth Matesanz,[⊥] José Fernando Díaz,[⊥] Anna Ivana Scovassi,[#] Ennio Prosperi,[#] Antonio Lavecchia,[⊗] Ettore Novellino,[⊗] Marino Artico,[†] and Romano Silvestri*[,†]

Istituto Pasteur − Fondazione Cenci Bolognetti, Dipartimento di Studi Farmaceutici, Sapienza Università di Roma, Piazzale Aldo Moro 5, I-00185 Roma, Italy, Welsh School of Pharmacy, Cardiff University, King Edward VII Avenue, Cardiff, CF10 3XF, United Kingdom, Toxicology and Pharmacology Branch, Developmental Therapeutics Program, Division of Cancer Treatment and Diagnosis, National Cancer Institute at Frederick, National Institutes of Health, Frederick, Maryland 21702, Dipartimento di Chimica Farmaceutica e Tossicologica, Università di Napoli "Federico II", Via Domenico Montesano 49, I-80131, Napoli, Italy, Centro de Investigaciones Biológicas, Consejo Superior de Investigaciones Cientificas, C/Ramiro de Maeztu 9, E-28040 Madrid, Spain, and Istituto di Genetica Molecolare − Consiglio Nazionale delle Ricerche, Via Abbiategrasso 207, I-27100 Pavia, Italy

Received December 27, 2006

The new arylthioindole (ATI) derivatives **10**, **14**−**18**, and **21**−**24**, which bear a halogen atom or a small size ether group at position 5 of the indole moiety, were compared with the reference compounds colchicine and combretastatin A-4 for biological activity. Derivatives **10**, **11**, **16**, and **21**−**24** inhibited MCF-7 cell growth with IC_{50} values <50 nM. A halogen atom (**14**−**17**) at position 5 caused a significant reduction in the free energy of binding of compound to tubulin, with a concomitant reduction in cytotoxicity. In contrast, methyl (**21**) and methoxy (**22**) substituents at position 5 caused an increase in cytotoxicity. Compound **16**, the most potent antitubulin agent, led to a large increase (56%) in HeLa cells in the G_2/M phase at 24 h, and at 48 h, 26% of the cells were hyperploid. Molecular modeling studies showed that, despite the absence of the ester moiety present in the previously examined analogues, most of the compounds bind in the colchicine site in the same orientation as the previously studied ATIs. Binding to β-tubulin involved formation of a hydrogen bond between the indole and Thr179 and positioning of the trimethoxy phenyl group in a hydrophobic pocket near Cys241.

Introduction

Microtubules have essential roles in vital cellular functions, such as motility, division, shape maintenance, and intracellular transport. Drugs that interact with tubulin, the protein subunit of microtubules, cause mitotic arrest, interfering with the dynamic equilibrium of these organelles by either inhibiting tubulin polymerization or blocking microtubule disassembly. Inhibitors of tubulin assembly include colchicine (**1**), combretastatin A-4 (CAS4, **2a**), and the *Catharanthus* alkaloids vincristine and vinblastine (Chart 1). At high concentrations, **1** and **2a** interact with α,β-tubulin dimers at the interface between alpha and beta[1] and cause microtubule destabilization and apoptosis. Taxoids and epothilones bind as well to α,β-tubulin to a lumenal site on the β-subunit[2,3] and probably to a recently described microtubule stabilizing agent binding site[4] in the pore on the microtubule surface formed by two different α and β tubulin subunits. Paclitaxel stimulates microtubule polymerization and stabilization at high concentrations, whereas at lower concentrations, the drug inhibits microtubule dynamics with little effect on the proportion of tubulin in polymer.[5,6] Independent of precise mechanism of action, clinical use of antitubulin drugs is associated with problems of drug resistance, toxicity, and bioavailability.[7]

Chart 1. Reference and Arylthioindole Derivatives

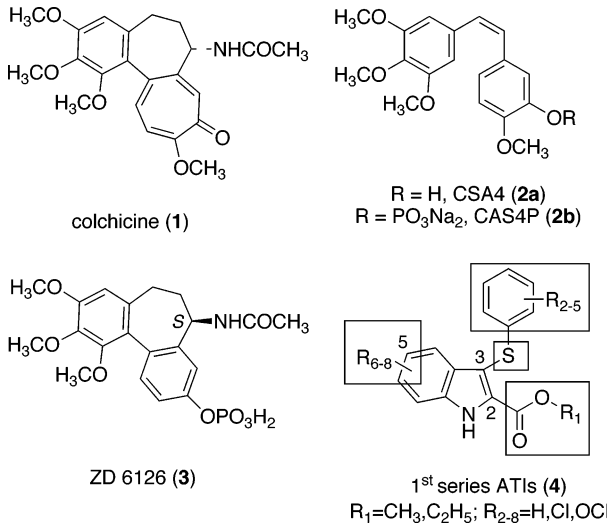

In the past few years, several antitubulin agents that target the colchicine site have been intensively investigated as vascular-disrupting antitumor drugs.[8] For example, combretastatin A-4 phosphate (**2b**) and ZD6126 (**3**) stop blood flow through tumor capillaries, probably caused by rapid disruption of endothelial cell morphology, and consequently, the tumor is starved of nutrients and rapid tumor cell death occurs.[9,10] These vascular-disrupting agents are currently in ongoing clinical trials for either single-drug or multi-drug combination antitumor therapy.[10,11]

Arylthioindoles (ATIs, general structure **4**) are a new class of potent tubulin assembly inhibitors that bind to the colchicine site on β-tubulin close to its interface with α-tubulin.[12]

* To whom correspondence should be addressed. Phone: +39 06 4991 3800. Fax: +39 06 491 491. E-mail: romano.silvestri@uniroma1.it.
† Università di Roma.
‡ Research performed at Cardiff University.
§ National Cancer Institute at Frederick.
∥ Cardiff University.
⊥ Consejo Superior de Investigaciones Cientificas, Madrid.
Consiglio Nazionale delle Ricerche, Pavia.
⊗ Università di Napoli.

10.1021/jm061479u CCC: $37.00
Published on Web 05/12/2007

Chart 2. Design of Arylthioindoles **9**−**28**

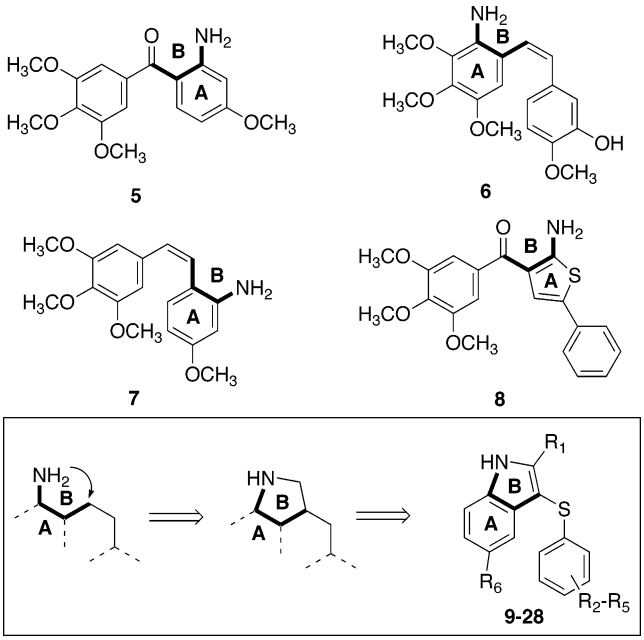

Structure−activity relationship (SAR) analysis clarified structural requirements for good activity in this class of inhibitors. Essential structural features for an active agent have included (A) a small-size ester function at position 2 of the indole, (B) the 3-arylthio group, (C) the sulfur atom bridge, and (D) a substituent at position 5 of the indole (Chart 1).[13] We carried out molecular modeling studies and dynamics simulations that helped explain the experimental data. We therefore used our molecular model in designing and synthesizing new ATI derivatives.[13]

Recent studies have focused on the synthesis of aminoderivatives related to CSA4.[14] The potent antitubulin activity displayed by these analogues (for example **5**,[15] **6**,[16] **7**,[16] and **8**[17], Chart 2) attracted our attention. Compounds **5**−**8** share, as a common structural feature, an amino group located *ortho* to the bridging group (either carbonyl or *cis*-ethenyl group). We hypothesized that this *ortho*-substituted aniline might resemble the indole nucleus of ATI derivatives (see Chart 2), with the indole ring acting as a bioisostere of the *ortho*-substituted aniline. These observations prompted us to design new ATI derivatives **9**−**28**. Predictive docking simulations using our model[13] showed that, despite the absence of the ester moiety at position 2 of the indole ring, most of the compounds should bind in the colchicine site of tubulin in the same orientation as the previously studied ATIs. The new ATI derivatives, like those described previously, were potent inhibitors of tubulin polymerization and of the growth of cancer cells, with activities comparable with those of colchicine and combretastatin A-4. Finally, we should note the recent paper of Hsieh and co-workers,[18] which included a group of 3-aroylthioindoles. These compounds are significantly different from the ATI's we have prepared, because there are major differences in our SAR findings and those of the Hsieh group.

Chemistry

The structures of ATI derivatives **9**−**31** are shown in Table 1. Compounds **10**, **11**, **14**−**26**, and **28** were synthesized by a two-step procedure (Scheme 1). *O*-Ethyl-*S*-(3,4,5-trimethoxyphenyl)carbonodithioate[19] was transformed into 3,4,5-trimethoxythiophenol by heating at 65 °C in aqueous ethanol in the presence of sodium hydroxide. This mixture was made acidic with 6 N HCl and treated at 25 °C with the appropriate indole while adding dropwise an aqueous iodine−potassium iodide

Table 1. Structures of ATIs **9**−**31**

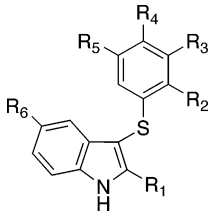

cmpd	R_1	R_2	R_3	R_4	R_5	R_6
9	H	H	H	H	H	H
10	H	H	OCH_3	OCH_3	OCH_3	H
11	CH_3	H	OCH_3	OCH_3	OCH_3	H
12	H	OCH_3	H	H	H	Cl
13	H	H	CH_3	H	CH_3	Cl
14	H	H	OCH_3	OCH_3	OCH_3	Cl
15	CH_3	H	OCH_3	OCH_3	OCH_3	Cl
16	H	H	OCH_3	OCH_3	OCH_3	Br
17	H	H	OCH_3	OCH_3	OCH_3	I
18	H	H	OCH_3	OCH_3	OCH_3	F
19	H	H	OCH_3	OCH_3	OCH_3	NO_2
20	H	H	OCH_3	OCH_3	OCH_3	NH_2
21	H	H	OCH_3	OCH_3	OCH_3	CH_3
22	H	H	OCH_3	OCH_3	OCH_3	OCH_3
23	CH_3	H	OCH_3	OCH_3	OCH_3	OCH_3
24	H	H	OCH_3	OCH_3	OCH_3	OCH_2CH_3
25	H	H	OCH_3	OCH_3	OCH_3	$OCH(CH_3)_2$
26	H	H	OCH_3	OCH_3	OCH_3	OH
27	H	H	OCH_3	OCH_3	OCH_3	OCH_2CH_2OH
28	H	H	OCH_3	OCH_3	OCH_3	$OCH_2CH_2OCH_2Ph$
29	$COOCH_3$	H	OCH_3	OCH_3	OCH_3	H
30	$COOCH_3$	H	OCH_3	OCH_3	OCH_3	Cl
31	$COOCH_3$	H	OCH_3	OCH_3	OCH_3	OCH_3

Scheme 1. Synthesis of Arylthioindole Derivatives **9**−**28**[a]

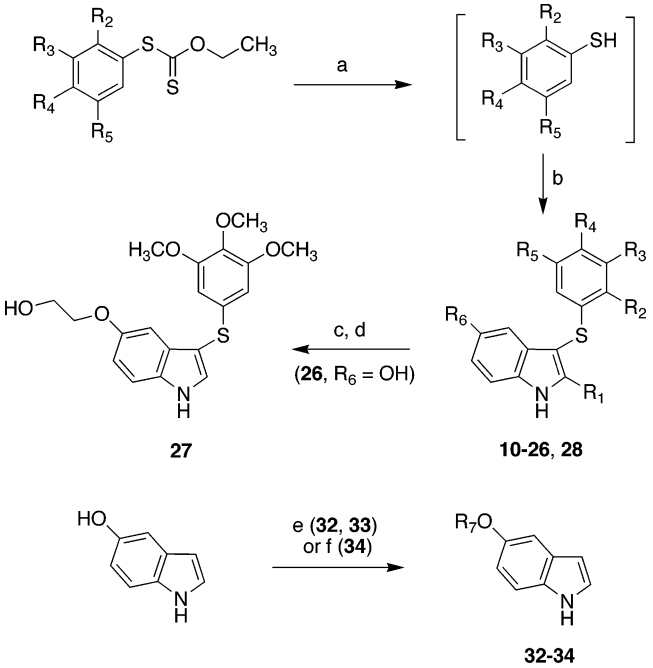

10-26, **28**: R_1= H, CH_3; $R_{2\text{-}5}$ = H, CH_3, OCH_3; R_6 = H, F, Cl, Br, I, NO_2, NH_2, OCH_3,OC_2H_5,$OCH(CH_3)_2$, OH, $OCH_2CH_2OCH_2Ph$. **32**: R_7 = C_2H_5; **33**: R_7 = $OCH(CH_3)_2$; **34**: R_7 = $OCH_2CH_2OCH_2Ph$.

[a] Reagents and reaction conditions: (a) 3 N NaOH, D-(+)-glucose, EtOH, 65 °C, 2 h; (b) appropriate indole, I_2-KI, EtOH−H_2O, 25 °C, 1 h; (c) (2-bromoethoxy)-*tert*-butyldimethylsilane, K_2CO_3, acetone, 24 h, reflux; (d) PTSA, methanol, 25 °C, 30 min; (e) alkyl halide, K_2CO_3, acetone, 24 h, reflux; (f) 2-benzyloxyethanol, DEAD, PPh_3, THF, overnight, reflux.

Table 2. Inhibition of Tubulin Polymerization, Growth of MCF-7 Human Breast Carcinoma Cells, and Colchicine Binding by Compounds **9**−**31**

cmpd	tubulin[a] $IC_{50} \pm SD$ (μM)	MCF-7[b] $IC_{50} \pm SD$ (nM)	inhibition colchicine binding[c] (% ± SD)
9[d]	15 ± 0.7	>2500	nd[e]
10	2.6 ± 0.2	34 ± 9	68 ± 0.8
11	6.8 ± 0.6	46 ± 4	61 ± 4
12	11 ± 2	>2500	nd
13	9.4 ± 0.3	1200 ± 100	33 ± 3
14	2.6 ± 0.2	77 ± 7	51 ± 4
15	2.7 ± 0.5	82 ± 10	59 ± 5
16	1.6 ± 0.3	43 ± 7	65 ± 3
17	2.7 ± 0.3	68 ± 7	61 ± 2
18	3.3 ± 0.3	160 ± 50	39 ± 6
19	16 ± 0.4	560 ± 70	nd
20	13 ± 2	260 ± 30	nd
21	2.7 ± 0.2	16 ± 6	56 ± 3
22	4.1 ± 0.6	22 ± 2	61 ± 4
23	3.3 ± 0.2	18 ± 4	69 ± 0.2
24	2.1 ± 0.1	16 ± 5	76 ± 5
25	19 ± 0.6	1500 ± 700	nd
26	6.3 ± 0.8	190 ± 40	26 ± 0.5
27	6.8 ± 0.8	95 ± 8	31 ± 2
28	>40	260 ± 20	nd
29[d]	2.9 ± 0.1	25 ± 1	74 ± 2
30[d]	2.3 ± 0.3	42 ± 1	57 ± 2
31[d]	2.0 ± 0.2	13 ± 3	90 ± 1
1	3.2 ± 0.4	13 ± 3	
2a	2.2 ± 0.2	17 ± 10	99 ± 1

[a] Inhibition of tubulin polymerization. [b] Inhibition of growth of MCF-7 human breast carcinoma cells.[20] [c] Inhibition of [^{3}H]colchicine binding. Tubulin was at 1 μM, both [^{3}H]colchicine and inhibitor were at 5 μM.[20] [d] Data from lit.[12,13] [e] nd = not determined.

solution. Compounds **12** and **13** were prepared similarly, starting from the corresponding commercially available carbonodithioate. Compound **27** was prepared by treating **26** with (2-bromoethoxy)-*tert*-butyldimethylsilane in the presence of potassium carbonate in boiling acetone; the intermediate silyloxy derivative was stirred with *para*-toluensulfonic acid in methanol at room temperature. The 5-ethoxy- (**32**) and 5-isopropyloxy- (**33**) indoles were obtained by alkylation of 5-hydroxyindole with iodoethane or 2-iodopropane, respectively, in the presence of potassium carbonate. 5-(2-Benzyloxy)ethoxyindole (**34**) was prepared by reaction of 5-hydroxyindole with 2-benzyloxyethanol in the presence of diethyl azodicarboxylate and triphenylphosphine in boiling THF.

Results and Discussion

Biological data for the inhibition of tubulin polymerization, binding of [^{3}H]colchicine to tubulin (more active compounds only), and growth of MCF-7 human breast carcinoma cells by arylthioindoles **9**−**28** in comparison with the reference compounds **1** and **2a** and ATIs **29**−**31**[12,13] are summarized in Table 2.

Replacing the 3-phenylthio of **9** with the 3-(3,4,5-trimethoxyphenyl)thio group (**10**) resulted in a 5.8-fold increase in inhibition of tubulin polymerization. This value (IC_{50} = 2.6 μM) was very close to those of **1** (IC_{50} = 3.2 μM) and **2a** (IC_{50} = 2.2 μM). Most importantly, this chemical modification resulted in great improvement in antiproliferative activity against MCF-7 cells. The IC_{50} obtained with **10** was 34 nM, a value only 2.6- and 2-fold higher than those obtained with reference compounds **1** (IC_{50} = 13 nM) and **2a** (IC_{50} = 17 nM), respectively. The 2-methyl group of **11** caused a 2.6-fold reduction in activity as an inhibitor of tubulin assembly (IC_{50} = 6.8 μM) relative to **10**, while inhibition of MCF-7 cell growth (IC_{50} = 46 nM) was only marginally affected.

Chart 3. Reference Structures for Binding Studies

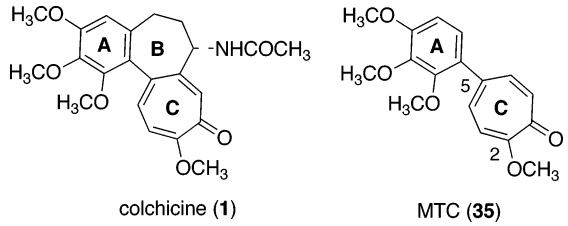

Introduction of a chlorine atom at position 5 of the indole (**14**, IC_{50} = 2.6 μM) did not change the activity of **10** as an inhibitor of assembly, but inhibition of cell growth was reduced greater than 2-fold. When a chlorine atom was introduced into **11** (compound **15**), inhibition of tubulin assembly increased while inhibition of MCF-7 cell growth decreased. (Alternatively, **15** can be viewed as an introduction of a C-2 methyl group into compound **14**, resulting in no change in activity, as compared with the loss of activity when the same methyl group was introduced into **10**.) With the other three halogen atoms (**16**−**18**), a bromine atom (**16**) resulted in a compound more inhibitory than **10** in the tubulin assembly assay and essentially identical to **10** as an inhibitor of MCF-7 cell growth, an iodine atom (**17**) was almost indistinguishable in its effects from the chlorine atom, and a fluorine atom (**18**) resulted in the least active compound in the halogen series, although with the latter compound there was a greater loss in antiproliferative than in antitubulin activity.

Introduction into **10** of a methyl (**21**, IC_{50} = 2.7 μM), a methoxy (**22**, IC_{50} = 4.1 μM; **23**, with a C-2 methyl group also, IC_{50} = 3.3 μM), or an ethoxy (**24**, IC_{50} = 2.1 μM) group at position 5 of the indole resulted in little change in inhibitory effect on tubulin assembly and small increases in antiproliferative activity relative to **10**. These compounds, too, were essentially equipotent with **1** and **2a**, both as inhibitors of tubulin assembly and MCF-7 cell growth. Bulkier ether groups at position 5 of the indole (**25**, **27**, **28**), or even a hydroxyl group at this position (**26**), yielded compounds with reduced activity in both assays.

In the assay measuring inhibition of [^{3}H]colchicine binding, all compounds were examined at 5 μM, with 1 μM tubulin and 5 μM **1**.[20] None of the new compounds approached the standard **2a** as an inhibitor in this assay. With the inhibitors at 1 μM, **2a** inhibited colchicine binding 88%, and the most active of the ATI's, compound **24**, inhibited 42%.

Structure−Affinity−Cytotoxicity Relationships. We also determined binding constants at 20 °C for the colchicine site on tubulin for the new ATIs that were highly active as inhibitors of tubulin polymerization. Inhibition of tubulin polymerization does not directly correlate with binding affinity. On the other hand, binding affinity can be an important parameter involved in cytotoxicity.[21−25]

Compounds **10**, **11**, **14**−**17**, **21**−**23**, **29**, and **30** were compared with **1** and 2-methoxy-5-(2,3,4-trimethoxyphenyl)-2,4,6-cycloheptatrien-1-one (MTC, **35**, Chart 3), an analogue of colchicine lacking the B ring that rapidly reaches an equilibrium in its binding reaction with tubulin (Table 3), while losing part of the free energy of binding due to the entropy contribution needed for the immobilization of the A and C rings in the site.[26] As expected from their cytotoxicities and their activities as inhibitors of [^{3}H]colchicine binding, the compounds bound tightly to the colchicine site of tubulin, as they displaced compound **35** already bound to the colchicine site (Figure 1).

We explored structure−affinity relationships of the substituents at positions 2 and 5 of the indole nucleus. Invariably, the

Table 3. Binding Constants at 20 °C of Compounds **10**, **11**, **14**−**17**, **21**−**23**, **29**, and **30** and the Reference Compounds **1** and **35** for the Colchicine Site on Tubulin

cmpd	binding constant ($\times 10^5$ M^{-1})	ΔG_{app} 20 °C (kJ mol^{-1})
10[a]	52.1 ± 2.8	−37.7 ± 0.1
11[a]	55.0 ± 3.0	−37.8 ± 0.1
14[a]	8.1 ± 0.3	−33.1 ± 0.1
15[a]	20.7 ± 2.4	−35.4 ± 0.3
16[a]	27.6 ± 1.3	−36.1 ± 0.1
17[a]	23.1 ± 2.1	−35.7 ± 0.2
21[a]	19.6 ± 0.5	−35.3 ± 0.1
22[a]	30.5 ± 1.9	−36.4 ± 0.1
23[a]	63.8 ± 1.6	−38.2 ± 0.1
29[b]	5.7 ± 0.4	−32.3 ± 0.2
30[b]	13 ± 2	−34.3 ± 0.3
35[c]	4.7 ± 0.3	−31.8 ± 0.2
1[c]	1600	−46.0

[a] Data obtained measuring compound **35** displacement from the binding site.[27] [b] Data measured using quenching of tubulin fluorescence.[28,29] [c] Data from lit.[28]

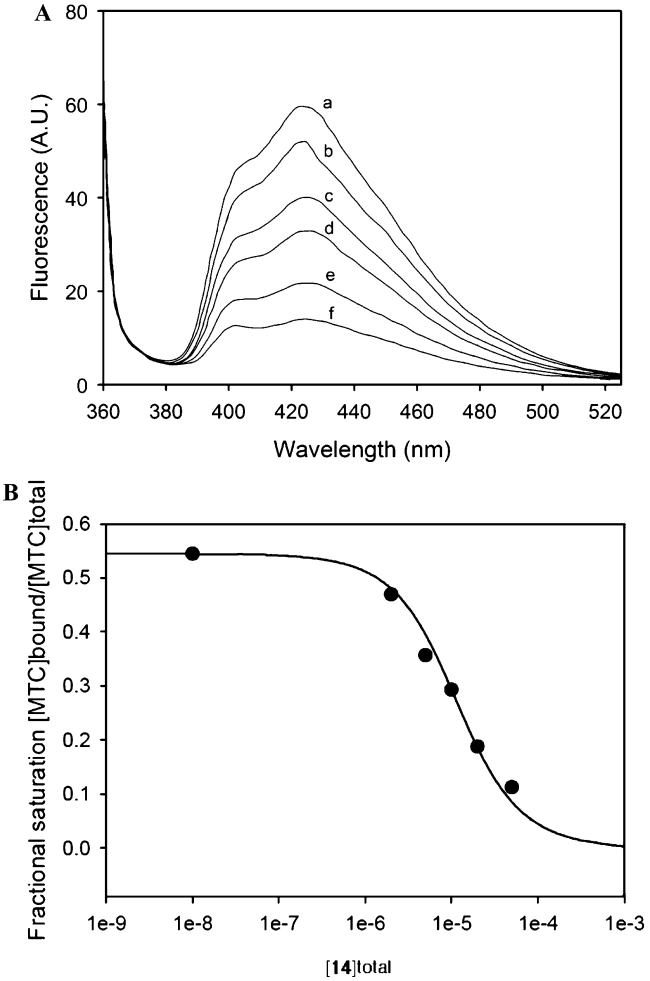

Figure 1. (A) Displacement of **35** from the colchicine site. Fluorescence emission spectra of 10 μM **35** and 10 μM tubulin in 10 mM phosphate−0.1 mM GTP buffer pH 7.0, in the presence of compound **14**: (a) 0 μM, (b) 2 μM, (c) 5 μM, (d) 10 μM, (e) 20 μM, (f) 50 μM. (B) Displacement isotherm at 20 °C of **35** by **14**. The data points were fit to the best value of the binding equilibrium constant of **14**, assuming 0.8 sites per tubulin dimer.[28]

presence of a halogen atom (**14**−**17**) or a methyl (**21**) or methoxy (**22**) group at position 5 resulted in reduction of binding affinity (positive value of $\Delta\Delta G$ 20 °C, Table 4). This reduction was accompanied by a concomitant reduction of cytotoxicity in **14**−**17** relative to **10**, while, in contrast, compounds **21** and **22** were more cytotoxic. The methyl group at position 2 increased binding affinity (negative value of $\Delta\Delta G$ 20 °C, Table 4), but this positive effect was not associated with an increase in cytotoxicity (compare **10** with **11** and **22** with **23**), probably due to a negative effect in solubility of the compound. The 2-methoxycarbonyl group of **29** and **30** caused opposite effects on the binding affinity of **10** and **14**, respectively. However, both **29** and **30** were more cytotoxic.

Table 4. Incremental Thermodynamic Parameters of Binding of Compounds **11**, **14**−**17**, **21**−**23**, **29** and **30** to the Colchicine Site

cmpd	reference cmpd	single group modification[a]	$\Delta\Delta G$ 20 °C (kJ mol^{-1})	MCF-7 ΔIC_{50} (nM)
11	**10**	2-**CH_3**	−0.1 ± 0.2	+12
14	**10**	5-**Cl**	+4.5 ± 0.2	+43
15	**11**	2-CH_3-5-**Cl**	+2.4 ± 0.4	+36
16	**10**	5-**Br**	+1.5 ± 0.2	+9
17	**10**	5-**I**	+1.9 ± 0.3	+34
21	**10**	5-**CH_3**	+2.3 ± 0.2	−18
22	**10**	5-**OCH_3**	+1.2 ± 0.2	−12
23	**22**	2-**CH_3**-5-CH_3O	−1.8 ± 0.2	−4
29	**10**	2-**$COOCH_3$**	+5.3 ± 0.2	−9
30	**14**	2-**$COOCH_3$**-5-Cl	−1.2 ± 0.4	−35
10	**35**		−5.8 ± 0.3	

[a] Single group modification (H → substituent) highlighted in bold on indole nucleus with respect to the indicated reference compound.

These results indicate that cytotoxicity is generally correlated with binding affinity for the colchicine site. However, some results were not fully explained in terms of binding affinity, suggesting that others factors, such as specific effects of the compound on the tubulin molecule,[22] may play a role in the cytotoxic activities of these derivatives.

We also analyzed the data from Table 2, combined with data from our previous studies,[12,13] comparing effects of ATIs on MCF-7 cell proliferation with inhibitory effects on tubulin assembly (Figure 2A) and with inhibitory effects on the binding of [^{3}H]colchicine to tubulin (Figure 2B). As noted above, assembly inhibition correlated poorly with inhibition of the growth of this cell line.

There was much better correlation with inhibition of colchicine binding, which indirectly measures relative affinity of the compounds for the colchicine site. Note, too, that **2a** and two compounds prepared by Flynn et al.[20] (previously cited by us[12]) also fit into the overall pattern generated by the ATIs.

Cell Cycle Analysis. The most potent antitubulin agent **16** was selected for cell cycle studies in HeLa cells. After treatment for 24 h with 0.1, 1.0, and 10 μM **16**, the cells showed a dose-dependent reduction in cell growth. At the highest concentration used, cell growth was reduced about 50% (not shown). Cell cycle analysis (Figure 3 and Table 5) following treatment with 10 μM **16** showed that 56% of the cells were arrested in the G_2/M phase after 24 h. Following replacement of the original medium with medium not containing the drug and incubation for a further 24 h, 53% of the cells remained in G_2/M and an additional 26% of the cells had DNA content >4C. These findings indicate a continuing impairment of cell division, as would be expected following treatment with a tubulin inhibitor.

The morphological features of **16**-treated cells were analyzed by Hoechst staining of cellular DNA. The nuclei of untreated HeLa cells showed the typical diffuse pattern of chromatin distribution, whereas cells treated with **16** became multinucleated as an effect of perturbation of tubulin function (Figure 4A). Although there was a small fraction of cells in the sub-G_1 region (the A_0 compartment in Table 5), other markers of apoptosis were not observed. There was neither a DNA ladder (Figure

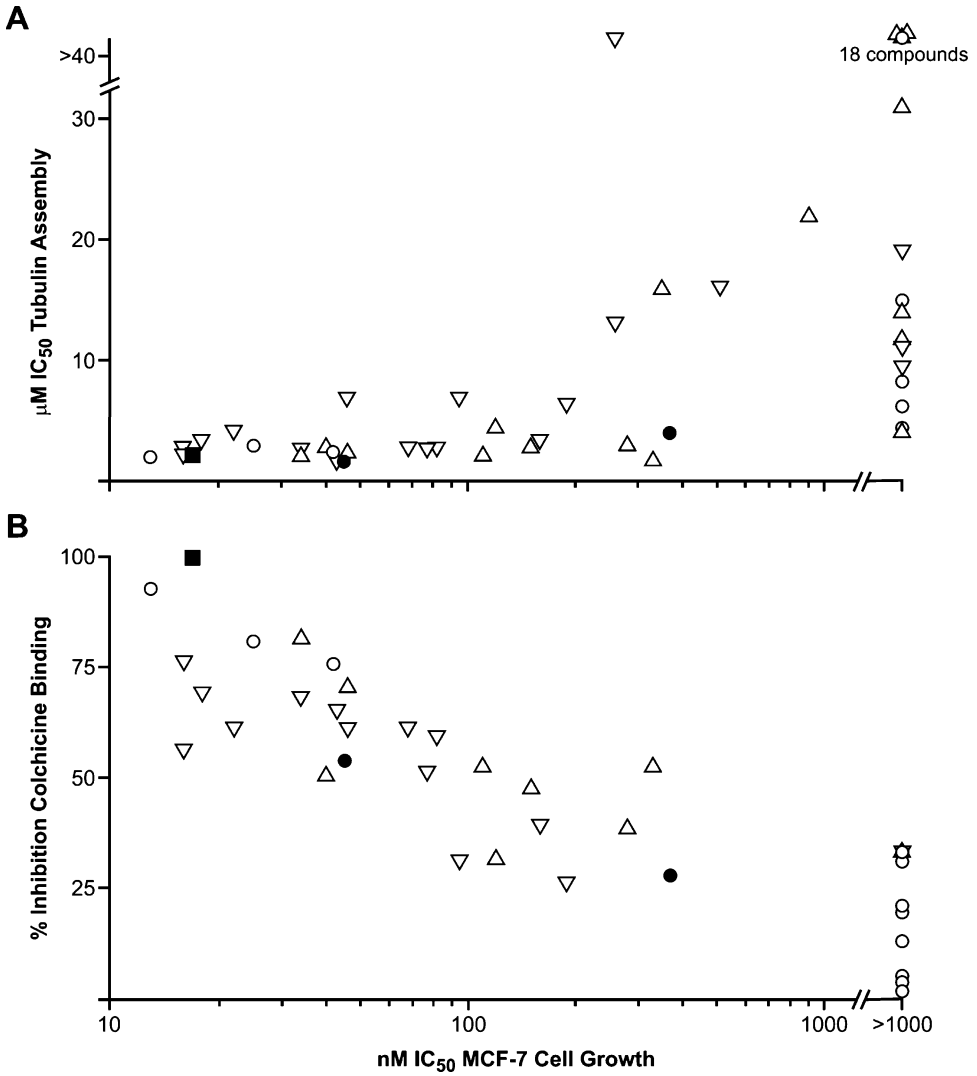

Figure 2. Correlation of MCF-7 cytotoxicity data with inhibition of tubulin assembly (A) and inhibition of colchicine binding (B). Data represented by open inverted triangles are taken from Table 2 of this paper. The open upright triangles represent ATI compounds described in ref 13 and the open circles represent ATI compounds described in ref 12. The solid squares represent data obtained with **2a**. The solid circles represent data obtained with two compounds synthesized by Flynn et al.[20]

4B) nor evidence for PARP-1 proteolysis (Figure 4C), both of which were instead observed following a 3 h treatment with etoposide.

These data suggested that tubulin polymerization inhibition induced in HeLa cells by **16** did not cause apoptosis but rather impaired cell viability through a "mitotic catastrophe".

Molecular Modeling. To investigate the possible binding mode for this new series of compounds, we performed docking simulations, using the FlexX module included in Sybyl 7.2.[30] We previously reported the putative binding for ATIs bearing an ester moiety at position 2 of the indole, describing the main interaction between the inhibitors and the colchicine site of tubulin, which included a hydrogen bond between the carbonyl group of the ester function and a lysine in the binding site.[12,13] With the series reported here, despite the absence of the ester moiety, most of the compounds bind in the same orientation as the previously studied ATIs, forming a hydrogen bond between the indole and Thr179 (residue numbers, as in ref 1, describing the crystal structure we used) and with the trimethoxyphenyl group positioned in a hydrophobic pocket close to Cys241 (Figure 5).

It should be noted that, while most of the compounds in this series dock in a very similar fashion, there are a few exceptions: compounds **9** and **10** showed a slightly different conformation, with the indole buried deeper in the binding pocket, although both compounds still form the interactions described above. In the case of compounds **19** and **28**, on the other hand, the docking simulation did not yield a reasonable pose within the active site. While with compound **28** it is possible to rationalize this observation as being caused by steric hindrance attributable to the substituent at position 5 of the indole, with compound **19**, the best explanation is that electrostatic effects cause a different positioning of the inhibitor in the binding site. If the conformation of compound **19** in the binding site was similar to the poses of the other analogues, its nitro group would be just 3 Å away from the phosphate groups of the nonexchangeable GTP molecule bound to the α-tubulin in the dimer. This GTP site on α-tubulin is near the colchicine site on β-tubulin, and the close proximity of the two ligands would result in an unacceptable electrostatic repulsion between negatively charged groups.

Conclusions

We synthesized new ATI derivatives, many of which strongly inhibited tubulin assembly, with activity in the low micromolar range, comparable to the effects of **1** and **2a**. Derivatives **10**,

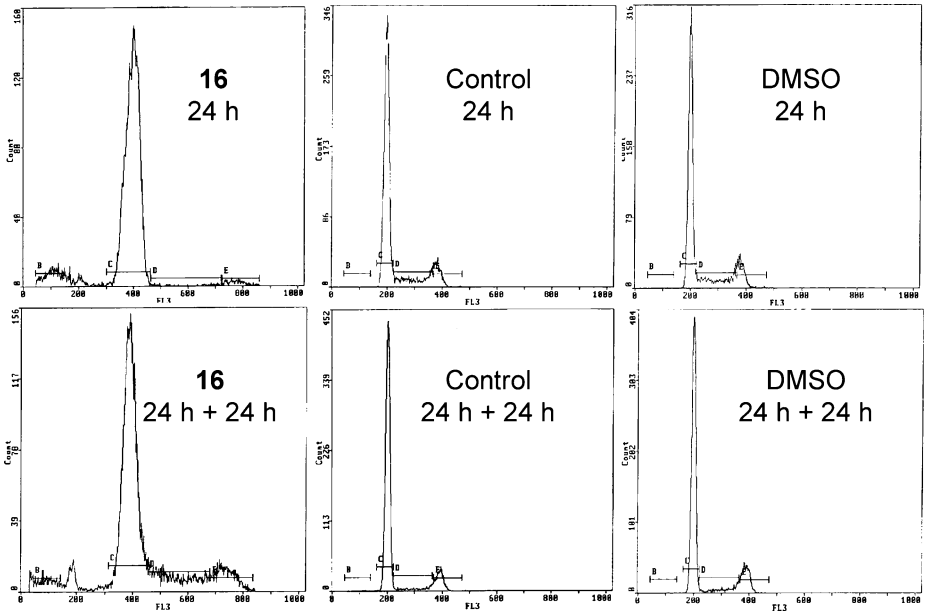

Figure 3. Cell cycle analysis of HeLa cells treated with **16**. A typical experiment is shown. Cells were harvested after treatment with **16** (10 μM) for 24 h and after further recovery in drug-free medium for 24 h (24 h + 24 h). The percentage of cells in each cell cycle phase was quantified (Table 5).

Table 5. Cell Cycle Distribution of **16**-Treated HeLa Cells[a]

cell cycle phase	24 h			24 h + 24 h		
	16[b]	control	DMSO[c]	**16**[d]	control	DMSO
A_0[e]	6.5	0.2	0.1	4.5	0.4	0.2
G_1	1.8	69.6	73.9	3.5	81.4	76.7
S	8.9	17.4	15.2	10.5	6.3	8.1
G_2/M	56.1	12.0	10.1	53.1	11.5	14.4
>4C	4.2	0	0	26.0	0	0

[a] Data are expressed as % of cells in each cell cycle phase. A typical experiment is shown. [b] Cells were treated with **16** at 10 μM for 24 h. [c] Parallel samples incubated with 0.1% DMSO (the same final concentration used with **16** at 10 μM) did not significantly alter cell cycle distribution. [d] Cells were further incubated in drug-free medium for 24 h. [e] Indicates cells with a sub-G_1 DNA content, probably representing a small population of apoptotic cells.

14−**18**, and **21**−**24**, bearing a halogen atom or a small alkyl or ether group at position 5 of the indole, were also potent inhibitors of MCF-7 cell growth. The most active derivatives (**10**, **11**, **16**, and **21**−**24**) inhibited cell growth with IC_{50} values <50 nM. SAR studies indicated reasonable, albeit imperfect, correlation between cytotoxicity and binding affinity for the colchicine site. In particular, a halogen atom at position 5 decreased the free energy of binding of ATIs to tubulin, with concomitant reduction in cytotoxicity. In contrast, methyl (**21**) and methoxy (**22**) substituents at position 5 resulted in more cytotoxic compounds. Compound **16**, the most potent inhibitor of tubulin assembly, induced accumulation of HeLa cells in the G_2/M phase of the cell cycle at 24 h and polyploidization at 48 h. At 24 h, inhibition of tubulin polymerization by **16** had not caused extensive apoptosis, suggesting that impaired cell viability might occur through a "mitotic catastrophe". Molecular modeling studies showed that, despite the absence of the ester moiety, most of the compounds appear to bind in the same orientation as the previously studied ATIs,[12,13] forming a hydrogen bond between the indole and Thr179 and with the trimethoxyphenyl group positioned in a hydrophobic pocket near Cys241. These findings induce us to continue our investigations of the SAR among ATI derivatives in the expectation of developing more potent and selective analogues.

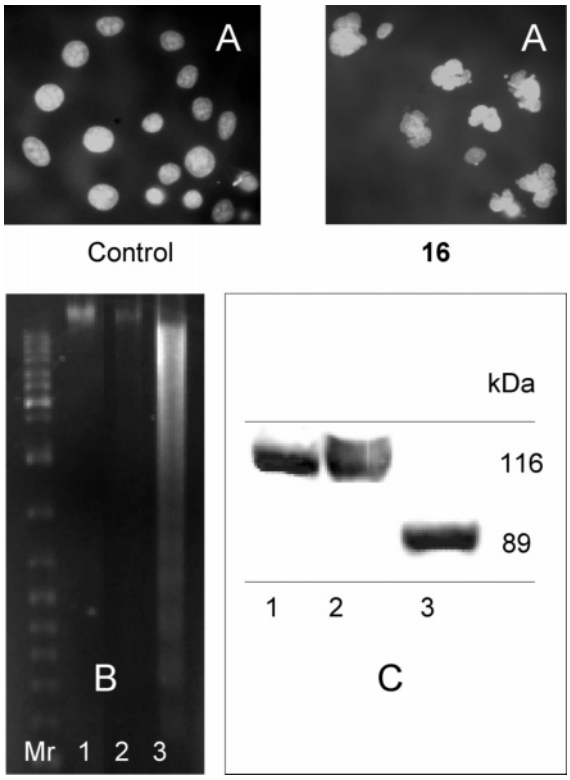

Figure 4. Morphological and biochemical evaluation of apoptotic parameters of HeLa cells treated with **16** and etoposide. (A) Hoechst staining for DNA. (B) Agarose gel electrophoresis; Mr, molecular weight markers; 1, control cells; 2, **16**-treated cells (10 μM, 24 h + 24 h of recovery); 3, etoposide-treated cells (100 μM, 3 h + 24 h of recovery). (C) Western blot for PARP-1; 1, control cells; 2, **16**-treated cells (10 μM, 24 h); 3, etoposide-treated cells (100 μM, 3 h + 24 h of recovery); 116 kDa, intact PARP-1; 89 kDa, caspase-cleaved PARP-1.

Experimental Section

Chemistry. Melting points (mp) were determined on a Büchi 510 apparatus and are uncorrected. Infrared spectra (IR) were run on a SpectrumOne FT spectrophotometer. Band position and absorption ranges are given in cm^{-1}. Proton nuclear magnetic

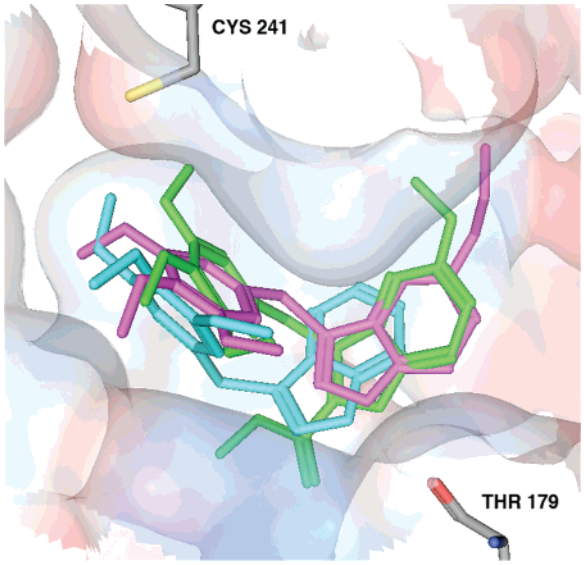

Figure 5. Putative binding mode of different ATIs: compound **31** in green, compound **24** in magenta, compound **10** in cyan.

resonance (^{1}H NMR) spectra were recorded on Bruker 200 and 400 MHz FT spectrometers in the indicated solvent. Chemical shifts are expressed in δ units (ppm) from tetramethylsilane. Mass spetra were recorded on Bruker MicroTOF LC. Column chromatography was performed on columns packed with alumina from Merck (70−230 mesh) or silica gel from Merck (70−230 mesh). Aluminum oxide TLC cards from Fluka (aluminum oxide precoated aluminum cards with fluorescent indicator at 254 nm) and silica gel TLC cards from Fluka (silica gel precoated aluminum cards with fluorescent indicator at 254 nm) were used for thin layer chromatography (TLC). Developed plates were visualized by a Spectroline ENF 260C/F UV apparatus. Organic solutions were dried over anhydrous sodium sulfate. Concentration and evaporation of the solvent after reaction or extraction was carried out on a Büchi Rotavapor rotary evaporator operating at reduced pressure. Elemental analyses were found within ±0.4% of the theoretical values. Compound **9** was synthesized as we previously reported.[12]

Method A. General Procedure for the Synthesis of Compounds 10−26 and 28. Example: 3-[(3,4,5-Trimethoxyphenyl)thio]-1*H*-indole (10). D-(+)-glucose (1.07 g, 0.006 mol) and 3 N NaOH (3.55 mL) were added to a solution of *O*-ethyl-*S*-(3,4,5-trimethoxyphenyl)carbonodithioate[19] (1.54 g, 0.005 mol) in ethanol (20 mL). The reaction mixture was heated at 65 °C for 2 h while stirring. After cooling, water (18 mL) and 6 N HCl (1.58 mL) were poured into the reaction mixture, and indole (0.5 g, 0.0043 mol) was added while stirring. A solution of iodine (1.08 g, 0.0043 mol) and potassium iodide (3.06 g, 0.02 mol) in water (11.5 mL) was dropped into the reaction, and it was stirred at 25 °C for 1 h. Water (20 mL) and a saturated solution of sodium hydrogen carbonate (15 mL) were added, and the mixture was extracted with chloroform. The organic layer was washed with brine, dried, and filtered. Evaporation of the solvent gave **10**, yield 47%, mp 125−128 °C (from ethanol). ^{1}H NMR (DMSO-d_6): δ 3.56 (s, 6H), 3.57 (s, 3H), 6.38 (s, 2H), 7.08 (t, J = 7.44 Hz, 1H), 7.18 (t, J = 7.56 Hz, 1H), 7.45 (d, J = 7.90 Hz, 1H), 7.48 (d, J = 8.07 Hz, 1H), 7.77 (s, 1H), 11.67 ppm (broad s, disappeared on treatment with D_2O, 1H). IR: ν 3356 cm^{-1}. MS: ES$^+$ = 338 (MNa$^+$). Anal. ($C_{17}H_{17}NO_3S$ (315.39)) C, H, N, S.

2-Methyl-3-[(3,4,5-trimethoxyphenyl)thio]-1*H*-indole (11). Compound **11** was synthesized as **10** using 2-methyl-1*H*-indole, yield 53%, mp 135−137 °C (from ethanol/water). ^{1}H NMR (DMSO-d_6): δ 2.44 (s, 3H), 3.57 (s, 9H), 6.29 (s, 2H), 7.03 (t, J = 7.03 Hz, 1H), 7.11 (t, J = 7.27 Hz, 1H), 7.37−7.39 (m, 2H), 11.61 ppm (broad s, disappeared on treatment with D_2O, 1H). IR: ν 3312 cm^{-1}. MS: ES$^+$ = 352 (MNa$^+$). Anal. ($C_{18}H_{19}NO_3S$ (329.42)) C, H, N, S.

5-Chloro-3-[(2-methoxyphenyl)thio]-1*H*-indole (12). Compound **12** was synthesized as **10** using 2-methoxythiophenol, yield 54%, mp 145−148 °C (from ethanol). ^{1}H NMR ($CDCl_3$): δ 3.97 (s, 3H), 6.59 (dd, J = 7.78 and 1.62 Hz, 1H), 6.68−6.72 (m, 1H), 6.86 (dd, J = 8.14 and 1.07 Hz, 1H), 7.05−7.09 (m, 1H), 7.22 (dd, J = 8.64 and 2.04 Hz, 1H), 7.37 (d, J = 8.63 Hz, 1H), 7.50 (d, J = 2.63 Hz, 1H), 7.60 (d, J = 2.02 Hz, 1H), 8.49 ppm (broad s, disappeared on treatment with D_2O, 1H). IR: ν 3433 cm^{-1}. MS: ES$^+$ = 312 (MNa$^+$). Anal. ($C_{15}H_{12}ClNOS$ (289.79)) C, H, Cl, N, S.

5-Chloro-3-[(3,5-dimethylphenyl)thio]-1*H*-indole (13). Compound **13** was synthesized as **10** using 3,5-dimethythiophenol and 5-chloro-1*H*-indole, yield 49%, mp 135−138 °C (from ethanol). ^{1}H NMR (DMSO-d_6): δ 2.12 (s, 6H), 6.66 (s, 2H), 6.70 (s, 1H), 7.18 (dd, J = 8.61 and 2.09 Hz, 1H), 7.35 (d, J = 2.06 Hz, 1H), 7.51 (d, J = 8.14 Hz, 1H), 7.83 (s, 1H), 11.89 ppm (broad s, disappeared on treatment with D_2O, 1H). IR: ν 3357 cm^{-1}. MS: ES$^+$ = 310 (MNa$^+$). Anal. ($C_{16}H_{14}ClNS$ (287.81)) C, H, Cl, N, S.

5-Chloro-3-[(3,4,5-trimethoxyphenyl)thio]-1*H*-indole (14). Compound **14** was synthesized as **10** using 5-chloro-1*H*-indole, yield 59%, mp 135−139 °C (from ethanol). ^{1}H NMR ($CDCl_3$): δ 3.68 (s, 6H), 3.79 (s, 3H), 6.36 (s, 2H), 7.20 (d, J = 8.73 Hz, 1H), 7.35 (d, J = 8.43 Hz, 1H), 7.51 (s, 1H), 7.62 (s, 1H) 8.69 ppm (broad s, disappeared on treatment with D_2O, 1H). IR: ν 3247 cm^{-1}. MS: ES$^+$ = 350 (MH$^+$). Anal. ($C_{17}H_{16}ClNO_3S$ (349.84)) C, H, Cl, N, S.

5-Chloro-2-methyl-3-[(3,4,5-trimethoxyphenyl)thio]-1*H*-indole (15). Compound **15** was synthesized as **10** using 5-chloro-2-methyl-1*H*-indole, yield 54%, mp 178−182 °C (from ethanol). ^{1}H NMR (DMSO-d_6): δ 2.48 (s, 3H), 3.59 (s, 9H), 6.28 (s, 2H), 7.12 (dd, J = 8.53 and 2.00 Hz, 1H), 7.32 (d, J = 4.68 Hz, 1H), 7.40 (d, J = 8.54 Hz, 1H), 11.84 ppm (broad s, disappeared on treatment with D_2O, 1H) IR: ν 3324 cm^{-1}. MS: ES$^+$ = 364 (MH$^+$). Anal. ($C_{18}H_{18}ClNO_3S$ (363.86)) C, H, Cl, N, S.

5-Bromo-3-[(3,4,5-trimethoxyphenyl)thio]-1*H*-indole (16). Compound **16** was synthesized as **10** using 5-bromo-1*H*-indole, yield 59%, mp 154−156 °C (from ethanol). ^{1}H NMR ($CDCl_3$): δ 3.70 (s, 6H), 3.82 (s, 3H), 6.39 (s, 2H), 7.31 (d, J = 8.60 Hz, 1H), 7.35 (dd, J = 8.64 and 1.82 Hz, 1H), 7.50 (d, J = 2.64 Hz, 1H), 7.80 (s, 1H) 8.82 ppm (broad s, disappeared on treatment with D_2O, 1H). IR: ν 3353 cm^{-1}. MS: ES$^+$ = 416, 418 (MNa$^+$). Anal. ($C_{17}H_{16}BrNO_3S$ (394.28)) C, H, Br, N, S.

5-Iodo-3-[(3,4,5-trimethoxyphenyl)thio]-1*H*-indole (17). Compound **17** was synthesized as **10** using 5-iodo-1*H*-indole, yield 60%, mp 178−180 °C (from ethanol). ^{1}H NMR ($CDCl_3$): δ 3.71 (s, 6H), 3.81 (s, 3H), 6.39 (s, 2H), 7.23 (d, J = 8.52 Hz, 1H), 7.47 (d, J = 2.65 Hz, 1H), 7.53 (dd, J = 8.54 and 1.66 Hz, 1H), 8.02 (s, 1H) 8.66 ppm (broad s, disappeared on treatment with D_2O, 1H). IR: ν 3354 cm^{-1}. MS: ES$^+$ = 464 (MNa$^+$). Anal. ($C_{17}H_{16}INO_3S$ (441.29)) C, H, I, N, S.

5-Fluoro-3-[(3,4,5-trimethoxyphenyl)thio]-1*H*-indole (18). Compound **18** was synthesized as **10** using 5-fluoro-1*H*-indole, yield 57%, mp 160−163 °C (from ethanol). ^{1}H NMR ($CDCl_3$): δ 3.68 (s, 6H), 3.78 (s, 3H), 6.37 (s, 2H), 6.98−7.04 (m, 1H), 7.29 (dd, J = 9.16 and 2.51 Hz, 1H), 7.35 (dd, J = 8.83 and 4.21 Hz, 1H), 7.54 (d, J = 2.68 Hz, 1H), 8.52 ppm (broad s, disappeared on treatment with D_2O, 1H). IR: ν 3344 cm^{-1}. MS: ES$^+$ = 356 (MNa$^+$). Anal. ($C_{17}H_{16}FNO_3S$ (333.38)) C, H, F, N, S.

5-Nitro-3-[(3,4,5-trimethoxyphenyl)thio]-1*H*-indole (19). Compound **19** was synthesized as **10** using 5-nitro-1*H*-indole, yield 6%, yellow oil. ^{1}H NMR (DMSO-d_6): δ 3.58 (s, 3H), 3.60 (s, 6H), 6.44 (s, 2H), 7.68 (d, J = 8.54 Hz, 1H), 8.06−8.09 (m, 2H), 8.32 (d, J = 2.33 Hz, 1H), 12.48 ppm (broad s, disappeared on treatment with D_2O, 1H). IR: ν 3284 cm^{-1}. MS: ES$^+$ = 383 (MNa$^+$). Anal. ($C_{17}H_{16}N_2O_5S$ (360.39)) C, H, N, S.

5-Amino-3-[(3,4,5-trimethoxyphenyl)thio]-1*H*-indole (20). Compound **20** was synthesized as **10** using 5-amino-1*H*-indole, yield 17%, mp 128−131 °C (from ethanol). ^{1}H NMR ($CDCl_3$): δ 3.60 (broad s, disappeared on treatment with D_2O, 2H), 3.69 (s, 6H), 3.79 (s, 3H), 6.38 (s, 2H), 6.72 (dd, J = 8.55 and 2.20 Hz, 1H), 6.91 (d, J = 2.17 Hz, 1H), 7.24 (d, J = 8.54 Hz, 1H), 7.42 (d, J =

2.66 Hz, 1H) 8.30 ppm (broad s, disappeared on treatment with D_2O, 1H). IR: ν 3393 cm^{-1}. MS: $ES^+ = 331$ (MH^+). Anal. ($C_{17}H_{18}N_2O_3S$ (330.41)) C, H, N, S.

5-Methyl-3-[(3,4,5-trimethoxyphenyl)thio]-1*H*-indole (21). Compound **21** was synthesized as **10** using 5-methyl-1*H*-indole, yield 45%, oil which solidified on standing, mp 81−84 °C (aqueous ethanol). ^1H NMR ($CDCl_3$): δ 2.45 (s, 3H), 3.69 (s, 6H), 3.83 (s, 3H), 6.40 (s, 2H), 7.10 (d, $J = 7.69$ Hz, 1H), 7.34 (d, $J = 8.24$ Hz, 1H), 7.45 (s, 1H), 7.48 (d, $J = 2.58$ Hz, 1H), 8.38 ppm (broad s, disappeared on treatment with D_2O, 1H). IR: ν 3346 cm^{-1}. MS: $ES^+ = 330$ (MH^+). Anal. ($C_{18}H_{19}NO_3S$ (329.42)) C, H, N, S.

5-Methoxy-3-[(3,4,5-trimethoxyphenyl)thio]-1*H*-indole (22). Compound **22** was synthesized as **10** using 5-methoxy-1*H*-indole, yield 30%, 99−101 °C (from ethanol). ^1H NMR (DMSO-d_6): δ 3.57 (s, 3H), 3.58 (s, 6H), 3.71 (s, 3H), 6.39 (s, 2H), 7.82 (dd, $J =$ 8.76 and 2.43 Hz, 1H), 6.90 (d, $J = 2.38$ Hz, 1H), 7.38 (d, $J =$ 8.76 Hz, 1H), 7.71 (d, $J = 2.70$ Hz, 1H), 11.54 ppm (broad s, disappeared on treatment with D_2O, 1H). IR: ν 3356 cm^{-1}. MS: $ES^+ = 368$ (MNa^+). Anal. ($C_{18}H_{19}NO_4S$ (345.42)) C, H, N, S.

5-Methoxy-2-methyl-3-[(3,4,5-trimethoxyphenyl)thio]-1*H*-indole (23). Compound **23** was synthesized as **10** using 5-methoxy-2-methyl-1*H*-indole, yield 29%, mp 138−142 °C (from ethanol). ^1H NMR (DMSO-d_6): δ 2.44 (s, 3H), 3.58 (s, 9H), 3.71 (s, 3H), 6.30 (s, 2H), 6.74 (dd, $J = 8.66$ and 2.43 Hz, 1H), 6.84 (d, $J =$ 2.20 Hz, 1H), 7.27 (d, $J = 8.68$ Hz, 1H), 11.48 ppm (broad s, disappeared on treatment with D_2O, 1H). IR: ν 3339 cm^{-1}. MS: $ES^+ = 382$ (MNa^+). Anal. ($C_{19}H_{21}NO_4S$ (359.45)) C, H, N, S.

5-Ethoxy-3-[(3,4,5-trimethoxyphenyl)thio]-1*H*-indole (24). Compound **24** was synthesized as **10** using 5-ethoxy-1*H*-indole (**32**), yield 31%, brown oil. ^1H NMR ($CDCl_3$): δ 1.41 (t, $J = 6.98$ Hz, 3H), 3.68 (s, 6H), 3.79 (s, 3H), 4.04 (q, $J = 6.99$ Hz, 2H), 6.38 (s, 2H), 6.92 (dd, $J = 8.79$ and 2.43 Hz, 1H), 7.08 (d, $J = 2.37$ Hz, 1H), 7.33 (d, $J = 8.78$ Hz, 1H), 7.47 (d, $J = 2.68$ Hz, 1H), 8.48 ppm (broad s, disappeared on treatment with D_2O, 1H). IR: ν 3337 cm^{-1}. MS: $ES^+ = 382$ (MNa^+). Anal. ($C_{19}H_{21}NO_4S$ (359.45)) C, H, N, S.

5-Isopropoxy-3-[(3,4,5-trimethoxyphenyl)thio]-1*H*-indole (25). Compound **25** was synthesized as **10** using 5-isopropoxy-1*H*-indole (**33**), yield 31%, brown oil. ^1H NMR (DMSO-d_6): δ 1.20 (d, $J =$ 6.00 Hz, 6H), 3.57 (s, 9H), 4.44−4.48 (m, 1H), 6.39 (s, 2H), 6.79 (dd, $J = 8.75$ and 2.36 Hz, 1H), 6.86 (d, $J = 1.87$ Hz, 1H), 7.36 (d, $J = 8.72$ Hz, 1H), 7.69 (d, $J = 2.66$ Hz, 1H), 11.51 ppm (broad s, disappeared on treatment with D_2O, 1H). IR: ν 3392 cm^{-1}. MS: $ES^+ = 396$ (MNa^+). Anal. ($C_{20}H_{23}NO_4S$ (373.43)) C, H, N, S.

5-Hydroxy-3-[(3,4,5-trimethoxyphenyl)thio]-1*H*-indole (26). Compound **26** was synthesized as **10** using 5-hydroxy-1*H*-indole, yield 28%, 184−186 °C (from ethanol). ^1H NMR ($CDCl_3$): δ 3.34 (s, 9H), 6.35 (s, 2H), 6.67 (dd, $J = 8.62$ and 2.30 Hz, 1H), 6.76 (d, $J = 3.21$ Hz, 1H), 7.27 (d, $J = 8.64$ Hz, 1H), 7.63 (d, $J = 2.70$ Hz, 1H), 8.83 (broad s, disappeared on treatment with D_2O, 1H), 11.37 ppm (broad s, disappeared on treatment with D_2O, 1H). IR: ν 3340, 3279 cm^{-1}. MS: $ES^+ = 354$ (MNa^+). Anal. ($C_{17}H_{17}NO_4S$ (331.39)) C, H, N, S.

5-[2-(Benzyloxy)ethoxy]-3-[(3,4,5-trimethoxyphenyl)thio]-1*H*-indole (28). Compound **28** was synthesized as **10** using 5-(2-(benzyloxy)ethoxy)-1*H*-indole (**34**), yield 35%, brown oil. ^1H NMR ($CDCl_3$): δ 3.68 (s, 6H), 3.79 (s, 3H), 3.85 (t, $J = 4.88$ Hz, 2H), 4.18 (t, $J = 4.83$ Hz, 2H), 4.65 (s, 2H), 6.38 (s, 2H), 6.98 (dd, $J =$ 8.80 and 2.43 Hz, 1H), 7.11 (d, $J = 2.32$ Hz, 1H), 7.30−7.40 (m, 6H), 7.48 (d, $J = 2.67$ Hz, 1H), 8.42 ppm (broad s, disappeared on treatment with D_2O, 1H). IR: ν 3334 cm^{-1}. MS: $ES^+ = 488$ (MNa^+). Anal. ($C_{26}H_{27}NO_5S$ (465.57)) C, H, N, S.

2-[3-[(3,4,5-Trimethoxyphenyl)thio]-1*H*-indol-5-yloxy]ethanol (27). (2-Bromoethoxy)-*tert*-butyldimethylsilane (0.17 g, 0.16 mL, 0.724 mmol) and potassium carbonate (0.1 g, 0.72 mmol) were added to a solution of **26** (0.2 g, 0.603 mmol) in acetonitrile (30 mL). The reaction was refluxed overnight. (2-Bromoethoxy)-*tert*-butyldimethylsilane (0.17 g, 0.16 mL, 0.724 mmol) and potassium carbonate (0.1 g, 0.72 mmol) were added, and the reaction was refluxed for an additional 12 h. After cooling, water (10 mL) was added, and the reaction mixture was extracted with ethyl acetate; the organic layer was washed with brine, dried, and filtered. Evaporation of the solvent gave 5-[2-(*tert*-butyldimethylsilyloxy)-ethoxy]-3-[(3,4,5-trimethoxy phenyl)thio]-1*H*-indole (yield 41% as a brown oil), which was used without further purification. To a solution of the latter compound (0.11 g, 0.225 mol) in methanol (1.13 mL) was added *para*-toluenesulfonic acid monohydrate (0.01 g, 0.05 mmol). The reaction mixture was stirred at 25 °C for 30 min, neutralized with a saturated solution of sodium hydrogen carbonate, and extracted with ethyl acetate; the organic layer was washed with brine, dried, and filtered. Evaporation of the solvent gave a residue that was purified by silica gel column chromatography (ethyl acetate−*n*-hexane 7:1 as eluent) to furnish **27**, yield 22%, as a yellow oil. ^1H NMR ($CDCl_3$): δ 2.19 (broad s, disappeared on treatment with D_2O, 1H), 3.69 (s, 6H), 3.80 (s, 3H), 3.94−3.99 (m, 2H), 4.10 (t, $J = 4.53$ Hz, 2H), 6.39 (s, 2H), 6.94 (dd, $J = 8.79$ and 2.43 Hz, 1H), 7.11 (d, $J = 2.26$ Hz, 1H), 7.33 (d, $J = 8.79$ Hz, 1H), 7.48 (d, $J = 2.68$ Hz, 1H), 8.65 ppm (broad s, disappeared on treatment with D_2O, 1H). IR: ν 3336 cm^{-1}. MS: $ES^+ = 398$ (MNa^+). Anal. ($C_{19}H_{21}NO_5S$ (375.45)) C, H, N, S.

5-Ethoxy-1*H*-indole (32). Iodoethane (1.23 g, 0.63 mL, 0.0079 mol) and potassium carbonate (1.46 g, 0.01 mol) were added to a solution of 5-hydroxy-1*H*-indole (0.7 g, 0.0053 mol) in acetone (49 mL). The reaction mixture was refluxed overnight. Iodoethane (1.23 g, 0.63 mL, 0.0079 mol) and potassium carbonate (1.46 g, 0.01 mol) were added, and the reaction mixture was stirred at the same temperature for an additional 12 h. After cooling, the reaction mixture was filtered, and the resulting solution was diluted with ethyl acetate (30 mL) and washed with 3 N NaOH. The organic layer was washed with brine and dried. Evaporation of the solvent gave a residue that was purified by silica gel column chromatography (chloroform as eluent) to furnish **32**, yield 64%, yellow oil. ^1H NMR ($CDCl_3$): δ 1.49 (t, $J = 6.98$ Hz, 3H), 4.12 (q, $J = 6.98$ Hz, 2H), 6.50−6.52 (m, 1H), 6.91 (dd, $J = 8.78$ and 2.12 Hz, 1H), 7.16−7.18 (m, 2H), 7.28 (d, $J = 8.78$ Hz, 1H), 8.08 ppm (broad s, disappeared on treatment with D_2O, 1H). IR: ν 3409 cm^{-1}.

5-Isopropoxy-1*H*-indole (33). Compound **33** was synthesized as **32** using 2-iodopropane, yield 25%, yellow oil. ^1H NMR ($CDCl_3$): δ 1.38 (d, $J = 6.08$ Hz, 6H), 4.55 (m, 6.00−6.07 Hz, 1H), 6.48−6.50 (m, 1H), 6.88 (dd, $J = 8.75$ and 2.36 Hz, 1H), 7.17−7.19 (m, 2H), 7.28 (d, $J = 8.14$ Hz, 1H), 8.09 ppm (broad s, disappeared on treatment with D_2O, 1H). IR: ν 3412 cm^{-1}.

5-[2-(Benzyloxy)ethoxy]-1*H*-indole (34). A solution of diethyl azodicarboxylate (40% in toluene, 0.64 g, 1.60 mL, 0.0037 mol) was added dropwise to a mixture of 2-benzyloxyethanol (0.56 g, 0.53 mL, 0.0037 mol), 5-hydroxy-1*H*-indole (0.5 g, 0.0037 mol), and anhydrous triphenylphosphine (0.97 g, 0.0037 mol) in anhydrous tetrahydrofuran (23 mL). The reaction mixture was refluxed overnight. After evaporation of the solvent, water (15 mL) and ethyl acetate (15 mL) were added; the organic layer was washed with brine and dried. Removal of the solvent gave a residue that was purified by silica gel column chromatography (chloroform as eluent) to furnish **34**, yield 82%, brown oil. ^1H NMR ($CDCl_3$): δ 3.89 (t, $J = 4.92$ Hz, 2H), 4.23 (t, $J = 4.93$ Hz, 2H), 4.69 (s, 2H), 6.48−6.50 (m, 1H), 6.93 (dd, $J = 8.79$ and 2.44 Hz, 1H), 7.15 (d, $J =$ 2.37 Hz, 1H), 7.18−7.19 (m, 1H), 7.30−7.43 (m, 6H), 8.10 ppm (broad s, disappeared on treatment with D_2O, 1H). IR: ν 3409 cm^{-1}.

Biology. Tubulin Assembly. The reaction mixtures contained 0.8 M monosodium glutamate (pH 6.6 with HCl in 2 M stock solution), 10 μM tubulin, and varying concentrations of drug. Following a 15 min preincubation at 30 °C, samples were chilled on ice, GTP to 0.4 mM was added, and turbidity development was followed at 350 nm in a temperature controlled recording spectrophotometer for 20 min at 30 °C. The extent of the reaction was measured. Full experimental details were previously reported.[31]

[^{3}H]Colchicine Binding Assay. The reaction mixtures contained 1.0 μM tubulin, 5.0 μM [^{3}H]colchicine, and 5.0 μM inhibitor and were incubated 10 min at 37 °C. Complete details were described previously.[32]

MCF-7 Cell Growth. The above paper[32] can also be referenced for methodology of MCF-7 cell growth.

Binding Constants of the Ligands. The binding constants of the ligands were measured at 20 °C either by displacement of compound **35**[27] in a Shimadzu RF540 fluorimeter, with 5 nm excitation and emission slits and with excitation at 350 nm and emission at 422 nm. To check if any fluorescence or inner filter effect could interfere with the assay results, the spectra of all compounds dissolved in ethanol were determined in a Hitachi U-2000 spectrophotometer. Only compound **30** showed absorbance at the excitation wavelength (350 nm) of compound **35**, as well as emission at 422 nm. Therefore, its binding constant was measured by quenching of the intrinsic fluorescence of tubulin.[28,29] The data were analyzed using the software package Equigra v5.[25]

Cell Culture. HeLa cells were grown at 37 °C in a humidified atmosphere containing 5% CO_2 in DMEM (GIBCO BRL, U.K.) supplemented with 10% fetal calf serum (Hyclone, NL), 100 U/mL of penicillin and streptomycin, and 2 mM glutamine (all reagents were from Celbio, Italy). Cells were trypsinized when subconfluent, seeded in T75 flasks at a concentration of 2.5×10^5 cells/mL in complete medium and treated with compound **16** at 0.1−10 μM for 24 h. Cells were harvested either immediately at the end of the treatment or after a further incubation in drug-free medium for 24 h. In some experiments, HeLa cells were treated with 100 μM etoposide for 3 h, followed by a 24 h recovery period.

Viability and Morphology Assays. Viability was assessed by staining cells with trypan blue. Permeable cells were counted in a hemocytometer and considered as nonviable. To evaluate cell morphology, cells grown on glass coverslips were fixed for 10 min in ice-cold 70% ethanol, washed several times with ice-cold PBS, and stained for 10 min at room temperature with 0.1 μg/mL Hoechst 33258 (Sigma). Samples were washed with PBS, mounted on a glass slide in a drop of Mowiol (Calbiochem, Inalco, Italy), and observed by fluorescence microscopy.

Cell Cycle Analysis. Cells were detached by careful trypsinization (to obtain single-cell suspensions to be processed for flow cytometry), then resuspended in cold 0.9% NaCl and fixed with cold 70% (final concentration) ethanol. Cells were stained in a solution of PBS containing 30 μg/mL propidium iodide and 2 mg/mL RNase A (Sigma) and analyzed with an Epics XL flow cytometer (Beckman-Coulter Corp., U.S.A.). At least 10 000 cells/sample were measured.

Evaluation of apoptosis. To investigate DNA degradation, cells were rinsed twice in cold PBS containing 5 mM EDTA. Genomic DNA was extracted from 2.5×10^6 cells and analyzed by agarose gel electrophoresis.[33] PARP-1 proteolysis was used as a marker of caspase activation. Total extracts for western blots were prepared from 2.5×10^6 cells. The western blot analysis was performed as previously reported[33] with the mAb C-2−10 against PARP-1 (Alexis, Vinci-Biochem, Italy). An HRP-conjugated antimouse IgG antibody (Sigma) was used as the secondary antibody. Visualization was performed by the ECL Detection System (Sigma).

Molecular Modeling. All molecular modeling studies were performed on a RM Innovator with Pentium IV 3 GHz processor, running Linux Fedora Core 4 using Molecular Operating Environment (MOE) 2006.08[34] and the FlexX module in Sybyl 7.2.[30] The structure of two tubulin dimers, cocrystalized with a stathmin-like domain and *N*-deacetyl-*N*-(2-mercaptoacetyl)-colchicine (DAMA-colchicine), was downloaded from the PDB data bank (http://www.rcsb.org/pdb/index.html; PDB code: 1SA0).[1] Ligand structures were built with MOE and minimized using the MMFF94x forcefield until a RMSD gradient of 0.05 kcal mol^{-1} $Å^{-1}$ was reached. The partial charges were automatically calculated and the structure was saved as a mol2 file. Docking experiments were carried out using the FlexX docking program of Sybyl 7.2. The DAMA-colchicine present between chain C and chain D of the structure was used to define the binding site, which included all residues within 6.5 Å of the crystallized ligand. The GTP molecule situated at the edge of the binding site on α-tubulin was included as a heteroatom file. DAMA-colchicine was automatically removed from the active site by the software before the docking simulation. The output of FlexX docking was visualized in MOE, and the scoring.svl script[35] was used to identify interaction types between ligand and protein.

Acknowledgment. G. La R. thanks Istituto Pasteur − Fondazione Cenci Bolognetti for his Borsa di Studio per Ricerche all'Estero. G. De M. thanks Italian Miur for her Progetto Mobilità Studiosi Italiani all'Estero. This research was funded by Istituto Pasteur − Fondazione Cenci Bolognetti and Università di Roma "La Sapienza", Ricerche di Ateneo. Authors also thank FIRC (Federazione Italiana per la Ricerca sul Cancro) for its contribution. This work was supported by Grants BFU2004-00358 from the Dirección General de Investigación Científica y Tecnológica (DGICYT) and CAM200520M061 from Comunidad Autonoma de Madrid. This research was also partially supported by a grant of the Fondazione Banca del Monte di Lombardia (Pavia, Italy) to A.I.S. For S.K. we would like to acknowledge the Embassy of the Arab Republic of Egypt for the award of a PhD scholarship.

Supporting Information Available: Elemental analyses of new derivatives **10**−**28**. This material is available free of charge via Internet at http//pubs.acs.org.

References

(1) Ravelli, R. B.; Gigant, B.; Curmi, P. A.; Jourdain, I.; Lachkar, S.; Sobel, A.; Knossow, M. Insight into tubulin regulation from a complex with colchicine and a stathmin-like domain. *Nature* **2004**, *428*, 198−202.
(2) Nogales, E.; Whittaker, M.; Milligan, R. A.; Downing, K. H. High-resolution model of the microtubule. *Cell* **1999**, *96*, 79−88.
(3) Nettles, J. H.; Li, H.; Cornett, B.; Krahn, J. M.; Snyder, J. P.; Downing, K. H. The binding mode of epothilone A on alpha, beta-tubulin by electron crystallography. *Science* **2004**, *305*, 866−869.
(4) Buey, R. M.; Calvo, E.; Barasoain, I.; Pineda, O.; Edler, M. C.; Matesanz, R.; Cerezo, G.; Vanderwal, C. D.; Day, B. W.; Sorensen, E. J.; Lopez, J. A.; Andreu, J. M.; Hamel, E.; Diaz, J. F. Cyclostreptin binds covalently to microtubule pores and lumenal taxoid binding sites. *Nat. Chem. Biol.* **2007**, *3*, 117−125.
(5) Lin, M. C.; Ho, H. H.; Pettit, G. R.; Hamel, E. Antimitotic natural products combretastatin A-4 and combretastatin A-2: Studies on the mechanism of their inhibition of the binding to colchicine to tubulin. *Biochemistry* **1989**, *28*, 6984−6991.
(6) Beckers, T.; Mahboobi, S. Natural, semisynthetic and synthetic microtubule inhibitors for cancer therapy. *Drugs Future* **2003**, *28*, 767−785.
(7) Sridhare, M.; Macapinlac, M. J.; Goel, S.; Verdier-Pinard, D.; Fojo, T.; Rothenberg, M.; Colevas, D. The clinical development of new mitotic inhibitors that stabilize the microtubule. *Anticancer Drugs* **2004**, *15*, 553−555.
(8) Jordan, M. A.; Wilson, L.; Microtubules as a target for anticancer drugs. *Nat. Rev. Cancer* **2004**, *4*, 253−265.
(9) Mealy, N. E.; Balcells, L. M. Drugs under development for the treatment of breast cancer. *Drugs Future* **2006**, *31*, 541−564.
(10) Davis, P. D.; Dougherty, G. J.; Blakey, D. C.; Galbraith, S. M.; Tozer, G. M.; Holder, A. L.; Naylor, M. A.; Nolan, J.; Stratford, M. R. L.; Chaplin, D. J.; Hill, S. A. ZD6126: A novel vascular-targeting agent that causes selective destruction of tumor vasculature. *Cancer Res.* **2002**, *62*, 7247−7253.
(11) Chaplin, D. J.; Horsman, M. R.; Siemann, D. W. Current development status of small-molecule vascular disrupting agents. *Curr. Opin. Invest. Drugs* **2006**, *7*, 522−528.
(12) De Martino, G.; La Regina, G.; Coluccia, A.; Edler, M. C.; Barbera, M. C.; Brancale, A.; Wilcox, E.; Hamel, E.; Artico, M.; Silvestri, R. Arylthioindoles, potent inhibitors of tubulin polymerization. *J. Med. Chem.* **2004**, *47*, 6120−6123.
(13) De Martino, G.; Edler, M. C.; La Regina, G.; Coluccia, A.; Barbera, M. C.; Barrow, D.; Nicholson, R. I.; Chiosis, G.; Brancale, A.; Hamel, E.; Artico, M.; Silvestri, R. Arylthioindoles, potent inhibitors of tubulin polymerization. 2. Structure−activity relationships and molecular modeling studies. *J. Med. Chem.* **2006**, *49*, 947−954.
(14) Tron, G. C.; Pirali, T.; Sorba, G.; Pagliai, F.; Busacca, S.; Genazzani, A. A. Medicinal chemistry of combretastatin A4: Present and future directions. *J. Med. Chem.* **2006**, *49*, 3033−3044.
(15) Liou, J.-P.; Chang, C.-W.; Song, J.-S.; Yang, Y.-N.; Yeh, C.-F.; Tseng, H.-Y.; Lo, Y.-K.; Chang, Y.-L.; Chang, C.-M.; Hsieh, H.-P. Synthesis and structure−activity relationship of 2-aminobenzophenone derivatives as antimitotic agents. *J. Med. Chem.* **2002**, *45*, 2556−2562.

(16) Chang, J.-Y.; Yang, M.-F.; Chang, C.-Y.; Chen, C.-M.; Kuo, C.-C.; Liou, J.-P. 2-Amino and 2′-aminocombretastatin derivatives as potent antimitotic agents. *J. Med. Chem.* **2006**, *49*, 6412−6415.

(17) (a) Romagnoli, R.; Baraldi, P. G.; Pavani, M. G.; Tabrizi, M. A.; Preti, D.; Fruttarolo, F.; Piccagli, L.; Jung, M. K.; Hamel, E.; Borgatti, M.; Gambari, R. Synthesis and biological evaluation of 2-amino-3-(3′,4′,5′-trimethoxybenzoyl)-5-aryl thiophenes as a new class of potent antitubulin agents. *J. Med. Chem.* **2006**, *49*, 3906−3915. (b) Romagnoli, R.; Baraldi, P. G.; Remusat, V.; Carrion, M. D.; Cara, C. L.; Preti, D.; Fruttarolo, F.; Pavani, M. G.; Tabrizi, M. A.; Tolomeo, M.; Grimaudo, S.; Balzarini, J.; Jordan, M. A.; Hamel, E. Synthesis and biological evaluation of 2-(3′,4′,5′-trimethoxybenzoyl)-3-amino 5-aryl thiophenes as a new class of tubulin inhibitors. *J. Med. Chem.* **2006**, *49*, 6425−6428.

(18) Liou, J.-P.; Chang, Y.-L.; Kuo, F.-M.; Chang, C.-W.; Tseng, H.-Y.; Wang, C.-C.; Yang, Y.-N.; Chang, J.-Y.; Lee, S.-J.; Hsieh, H.-P. Concise synthesis and structure−activity relationships of combretastatin A-4 analogues, 1-aroylindoles and 3-aroylindoles, as novel classes of potent antitubulin agents. *J. Med. Chem.* **2004**, *47*, 4247−4257.

(19) Offer, J.; Boddy, C. N. C.; Dawson, P. E. Extending synthetic access to proteins with a removable acyl transfer auxiliary. *J. Am. Chem. Soc.* **2002**, *124*, 4642−4646.

(20) Flynn, B. L.; Flynn, G. P.; Hamel, E.; Jung, M. K. The synthesis and tubulin binding activity of thiophene-based analogues of combretastatin A-4. *Bioorg. Med. Chem. Lett.* **2001**, *11*, 2341−2343.

(21) Perez-Ramirez, B.; Shearwin, K. E.; Timasheff, S. N. The colchicine-induced GTPase activity of tubulin: State of the product. Activation by microtubule-promoting cosolvents. *Biochemistry* **1994**, *33*, 6253−6261.

(22) Perez-Ramirez, B.; Andreu, J. M.; Gorbunoff, M. J.; Timasheff, S. N. Stoichiometric and substoichiometric inhibition of tubulin self-assembly by colchicine analogues. *Biochemistry* **1996**, *35*, 3277−3285.

(23) Barbier, P.; Peyrot, V.; Leynadier, D.; Andreu, J. M. The active GTP- and ground GDP-liganded states of tubulin are distinguished by the binding of chiral isomers of ethyl 5-amino-2-methyl-1,2-dihydro-3-phenylpyrido[3,4-*b*]pyrazin-7-yl carbamate. *Biochemistry* **1998**, *37*, 758−768.

(24) Buey, R. M.; Diaz, J. F.; Andreu, J. M.; O'Brate, A.; Giannakakou, P.; Nicolaou, K. C.; Sasmal, P. K.; Ritzen, A.; Namoto, K. interaction of epothilone analogs with the paclitaxel binding site; relationship between binding affinity, microtubule stabilization, and cytotoxicity. *Chem. Biol.* **2004**, *11*, 225−236.

(25) Buey, R. M.; Barasoain, I.; Jackson, E.; Meyer, A.; Giannakakou, P.; Paterson, I.; Mooberry, S.; Andreu, J. M.; Diaz, J. F. Microtubule interactions with chemically diverse stabilizing agents: Thermodynamics of binding to the paclitaxel site predicts cytotoxicity. *Chem. Biol.* **2005**, *12*, 1269−1279.

(26) Medrano, F. J.; Andreu, J. M.; Gorbunoff, M. J.; Timasheff, S. N. Roles of colchicine rings B and C in the binding process to tubulin. *Biochemistry* **1989**, *28*, 5589−5599.

(27) Medrano, F. J.; Andreu, J. M.; Gorbunoff, M. J.; Timasheff, S. N. Roles of ring C oxygens in the binding of colchicine to tubulin. *Biochemistry* **1991**, *30*, 3770−3777.

(28) Andreu, J. M.; Gorbunoff, M. J.; Lee, J. C.; Timasheff, S. N. Interaction of tubulin with bifunctional colchicine analogues: An equilibrium study. *Biochemistry* **1984**, *23*, 1742−1752.

(29) Andreu, J. M.; Timasheff, S. N. Conformational states of tubulin liganded to colchicine, tropolone methyl ether, and podophyllotoxin. *Biochemistry* **1982**, *21*, 6465−6476.

(30) Tripos, *Sybyl 7.2*; Tripos Inc.: 1699 South Hanley Rd, St. Louis, Missouri 63144, http://www.tripos.com.

(31) Hamel, E. Evaluation of antimitotic agents by quantitative comparisons of their effects on the polymerization of purified tubulin. *Cell Biochem. Biophys.* **2003**, *38*, 1−21.

(32) Verdier-Pinard, P.; Lai, J.-Y.; Yoo, H.-D.; Yu, J.; Marquez, B.; Nagle, D. G.; Nambu, M.; White, J. D.; Falck, J. R.; Gerwick, W. H.; Day, B. W.; Hamel, E. Structure−activity analysis of the interaction of curacin A, the potent colchicine site antimitotic agent, with tubulin and effects of analogs on the growth of MCF-7 breast cancer cells. *Mol. Pharmacol.* **1998**, *53*, 62−76.

(33) Donzelli, M.; Bernardi, R.; Negri, C.; Prosperi, E.; Padovan, L.; Lavialle, C.; Brison, O.; Scovassi, A. I. Apoptosis-prone phenotype of human colon carcinoma cells with a high level amplification of the c-*myc* gene. *Oncogene* **1999**, *18*, 439−448.

(34) Molecular Operating Environment (MOE 2006.08); Chemical Computing Group, Inc.: Montreal, Quebec, Canada, http://www.chemcomp.com.

(35) Code "scoring.svl" obtained from the SLV Exchange website http://svl.chemcomp.com., Chemical Computing Group, Inc., Montreal, Canada.

JM061479U